MARCEL (inter-Modality Affine Registration with CorrELation ratio): An Application for Brain Shift Correction in Ultrasound-Guided Brain Tumor Resection

Nima Masoumi[1,2], Yiming Xiao[1,2], and Hassan Rivaz[1,2]

[1] PERFORM Centre, Concordia University, Montreal, Canada,
[2] Department of Electrical and Computer Engineering, Concordia University, Montreal, Canada
n_masoum@encs.concordia.ca

Abstract. Tissue deformation during brain tumor removal often renders the original surgical plan invalid. This can greatly affect the quality of resection, and thus threaten the patient's survival rate. Therefore, correction of such deformation is needed, which can be achieved through image registration between pre- and intra-operative images. We proposed a novel automatic inter-modal affine registration technique based on the correlation ratio (CR) similarity metric. The technique was demonstrated through registering intra-operative ultrasound (US) scans with magnetic resonance (MR) images of patients, who underwent brain gliomas resection. By using landmark-based mean target registration errors (TRE) for evaluation, our technique has achieved a result of 2.32±0.68 mm from the initial 5.13±2.78 mm.

1 Introduction

Gliomas are tumors in glial cells occurring either in brain or spine, and are currently the most common types of brain tumors in adults [1]. According the world health organization (WHO), brain gliomas can be classified into four different grades: low grade (Grade I and II) and high-grade (Grade III and IV). Low-grade gliomas (LGG) have a slower tumor growth rate, but will eventually progress to the deadlier high-grade tumors. Thus, early tumor removal can increase patient's survival rate [2].

During brain surgery, brain deforms to some extent, which is called brain shift and is caused by multiple reasons such as physiological factors [3]. Therefore, image guided neurosurgery systems (IGNS) that do not take brain shift into account can often render the pre-surgical plans invalid and can lead to incomplete or unnecessary resection.

Acquiring Magnetic Resonance Imaging (MRI) intra-operatively is difficult and requires special surgical tools and setups. Therefore, intra-operative ultrasound (US) has become popular due to its portability and non-invasiveness in recent years. The drawbacks with US are the low image quality and difficulty in interpreting the image contents. In order to track the surgical progress and brain shift, US images can be registered to pre-operative MRI to help recover the tissue deformation during operation [4]. Both T1-weighted MRI and T2-FLAIR

MRI are rountinely acquired for planning brain tumor resection procedures. However, low-grade gliomas are often more distinguishable in T2-FLAIR than in T1-weighted MRI [5].

Intensity based registration techniques need a similarity metric to evaluate similarities between two images. In these techniques, the goal of the registration is maximization of the similarity metric. Among popular similarity metrics, mutual information (MI) is the most general one and assumes statistical relationship between images. On the contrary, normalized cross-correlation (NCC) and sum of squared differences (SSD) assume linear relationship between images and are more restrictive. Correlation ratio (CR) assumes functional relationship between images, and provides enough generality to be used as a similarity metric between US and MRI [6, 7, 8]. In [7] automatic multimodal deformable registration performed with utilization of a modified version of CR. They also proposed a robust method for dealing with resected tumor [9].

Deformable registration problems, usually have much more parameters than affine and rigid registration, which respectively have twelve and six parameters. As a result, they usually have more accurate registration. However, in practice, affine registration has a lower chance of failure and is generally less computationally intensive.

In this paper, we introduced an automatic affine registration method using Robust paTch based cOrrelation Ration (RaPTOR) [7] to help recover brain shift using intra-operative US and pre-operative MRI scans. We used REtroSpective Evaluation of Cerebral Tumors (RESECT) database [5] to validate our method.

2 Materials and Methods

2.1 Registration Overview

Let I_f and I_m be respectively fixed and moving images. In the context of IGNS, we set I_f to the pre-operative MRI, and deform the intra-operative US image I_m towards the pre-operative MRI. We formulate the registration process as an optimization problem. Our cost C is defined in Eq. 1:

$$C = D(I_f(\mathbf{x}), I_m(\mathbf{T}(\mathbf{x}))) \tag{1}$$

where D is our objective function that should be minimized, I_f is the fixed image, I_m is the moving image, $\mathbf{x}$ is the point of interest in space, and $\mathbf{T}$ is the affine transformation matrix. The affine transformation matrix is defined in Eq. 2:

$$\boldsymbol{T} = \begin{bmatrix} a_1 & a_2 & a_3 & a_4 \\ a_5 & a_6 & a_7 & a_8 \\ a_9 & a_{10} & a_{11} & a_{12} \\ 0 & 0 & 0 & 1 \end{bmatrix} \tag{2}$$

where a_i, $1 \leq i \leq 12$ denotes the twelve affine transformation parameters. If $\mathbf{x} = [x_i,\ x_j,\ x_k]$ denotes the position of a point in Cartesian coordinates, we employ the transformation as in Eq. 3:

$$\begin{bmatrix} y_i \\ y_j \\ y_k \\ 1 \end{bmatrix} = \boldsymbol{T}(\boldsymbol{x}) = \boldsymbol{T} \times \begin{bmatrix} x_i \\ x_j \\ x_k \\ 1 \end{bmatrix} \tag{3}$$

where $\mathbf{y} = [y_i,\ y_j,\ y_k]$ specifies the transformed point. We define the objective function D as a dissimilarity metric in Eq. 4. The dissimilarity metric is RaPTOR (Robust PaTch based cOrrelation Ratio), which is modified version of CR (Correlation Ratio) [7].

$$D(Y,X) = RaPTOR(X,Y) = \frac{1}{N_p}\sum_{i=1}^{N_p}(1-\eta(Y|X;\boldsymbol{\Omega_i})) \tag{4}$$

In Eq. 4, N_P is the number of patches, $\boldsymbol{\Omega_i}$ is the set of all voxels included in patch i, and η is CR. D varies between 0 and 1. In higher similarity, D is closer to 0 and in lower similarity D is closer to 1.

The definition of CR in Eq. 4 is as following:

$$1-\eta(Y|X) = \frac{1}{N\sigma^2}\left(\sum_{t=1}^{N} i_t^2 - \sum_{j=1}^{N_b} N_j\mu_j^2\right) \tag{5}$$

$$\mu_j = \frac{\sum_{t=1}^{N}\lambda_{t,j}i_t}{N_j}, N_j = \sum_{t}\lambda_{t,j} \tag{6}$$

where N is total number of samples in Y, $\sigma^2 = Var[Y]$, i_t is the intensity of voxel number t in Y, N_b is the total number of bins, and $\lambda_{t,j}$ is the contribution of sample t in bin j as explained in [7].

2.2 Optimization and Outlier Suppression

We calculated the derivation of objective function analytically in order to speed up the registration procedure. We used derivative of the cost function in two distinct part. First in outlier suppression part. Second in updating equation of the optimization part.

Derivative of the cost function with respect to affine transformation parameters is as following:

$$\frac{\partial D}{\partial \mathbf{a}} = \left[\tfrac{\partial D}{\partial a_1}\ \tfrac{\partial D}{\partial a_2}\ \cdots\ \tfrac{\partial D}{\partial a_{12}}\right]^T \tag{7}$$

In Eq. 7, $\mathbf{a}$ is a vector consisting of affine transformation parameters. Now the derivative with respect to each of the parameters is:

$$\frac{\partial D}{\partial a_k} = \frac{1}{N_p}\sum_{i=1}^{N_p}\frac{\partial(1-\eta(Y|X;\boldsymbol{\Omega_i}))}{\partial a_k} \tag{8}$$

where $a_k,\ 1 \le k \le 12$ declares affine transformation parameters. Utilizing the chain rule, we have:

$$\frac{\partial(1-\eta(Y|X;\boldsymbol{\Omega_i}))}{\partial a_k} = \frac{\partial(1-\eta)}{\partial a_k} = \frac{\partial(1-\eta)}{\partial I_m(\mathbf{T}(\mathbf{x}))}.\frac{I_m(\mathbf{T}(\mathbf{x}))}{\partial \mathbf{d}}.\frac{\partial \mathbf{d}}{\partial a_k} \tag{9}$$

where $\mathbf{d} = [d_x, d_y, d_z]$ in Eq. 9 is the displacement vector in Cartesian coordinates. Right hand side of Eq. 9 has three terms. The first term was calculated in [7]. In order to comply with our equations, we bring up the calculation in

following equations. Note that the first term in Eq. 9 is the size of transformed moving image and we consider each element of this term as in Eq. 10 using Eq. 5.

$$\begin{gathered}\frac{\partial(1-\eta)}{\partial i_t} = \frac{\partial}{\partial i_t}\left(\frac{1}{N\sigma^2}\left(\sum_{k=1}^{N} i_k^2 - \sum_{j=1}^{N_b} N_j \mu_j^2\right)\right) = \\ \frac{-2(N-1)}{N^3\sigma^4}(i_t-\mu)\left(\sum_{k=1}^{N} i_k^2 - \sum_{j=1}^{N_b} N_j \mu_j^2\right) + \\ 2(i_t - \sum_{j=1}^{N_b} \mu_j \lambda_{t,j})(\frac{1}{N\sigma^2})\end{gathered} \tag{10}$$

In Eq. 10 μ is mean of Y. Second term in right hand side of Eq. 9 is simply the gradient of transformed moving image and third term is Jacobian of transformation.

Mini-Batch Gradient Descent Optimization: While batch gradient descent is time consuming and stochastic gradient descent (SGD) doesn't have required accuracy, choice of mini-batch gradient descent gives a trade-off between implementation time and result accuracy. For a certain resolution of input images, we select a set of random patches from the images in every iteration.

We employ Gaussian pyramid in the optimization. There are three pyramid levels in our analysis excluding the original size of images. In order to enable the dissimilarity metric to have a better perception of similarities between two input images, we select the set size of patches proportional to the resolution and size of input images in each level. Note that increasing the set size of patches will increase the computation time. Thus selecting the set size of patches in each pyramid level is a compromise between accuracy and computation time. The update equation for mini-batch gradient descent is as Eq. 11:

$$\boldsymbol{a_n} = \boldsymbol{a_{n-1}} - \alpha_n \frac{\partial D}{\partial \boldsymbol{a_{n-1}}} \tag{11}$$

where a_n is the vector consisting of affine transformation parameters in n-th iteration, $\frac{\partial D}{\partial \boldsymbol{a_n}}$ can be achieved by Eq. 7, and α_n is step size. Step size is a function of iteration number and is defined in Eq. 12.

$$\alpha_n = \frac{a}{(A+n)^\tau} \tag{12}$$

In Eq. 12 $a > 0$, $A \geq 0$, $0 < \tau \leq 1$ are constants. Klein et. al. [8] suggested approximate values for these parameters. According to [8], we set $a = 0.001$, $A = 0.3 \times MaxIterations$, and $\tau = 0.65$.

In comparison to the MRI, US has quite unique image features and its own challenges. The inherent properties of the ultrasound images can have a major effect on performance of the dissimilarity metric. Since we select patches in each iteration randomly, before any operation on the selected patches, we should preselect the patches that have potent image features (e.g., consistent and strong lines). We used outlier suppression proposed in [7]. We discard patches that are greater than a threshold T in Eq. 13.

$$r.r_g > T \tag{13}$$

Heuristically, $T = 1$ gives acceptable results for us. Parameter r is defined in Eq. 14.

$$r = min\left\{ \frac{Var(\frac{\partial D}{\partial d_x})}{\langle \frac{\partial D}{\partial d_x} \rangle^2}, \frac{Var(\frac{\partial D}{\partial d_y})}{\langle \frac{\partial D}{\partial d_y} \rangle^2}, \frac{Var(\frac{\partial D}{\partial d_z})}{\langle \frac{\partial D}{\partial d_z} \rangle^2} \right\} \tag{14}$$

where $\frac{\partial D}{\partial d_x}$, $\frac{\partial D}{\partial d_y}$, and $\frac{\partial D}{\partial d_z}$ are derivatives in x, y, and z direction respectively and $\langle . \rangle$ is mean operator. The denominators are low at relatively uniform regions, but are high in textured regions (i.e., with high gradients). Definition of r_g in Eq. 13 can be found in Eq. 15.

$$r_g = \frac{\|\nabla I_f\| * B}{\|\nabla I_m\| * B} \tag{15}$$

Here ∇ is gradient operator, $\|.\|$ indicates magnitude of the gradient, $*$ is convolution, and B is a kernel of size of the image with all ones in the selected patch and zeros the rest. The nominator and denominator represent summation of gradient values of fixed and moving image respectively.

2.3 Patient Data

To validate the proposed technique, we employed the MRI and intra-operative US scans of five patients, who underwent brain tumor resection procedures. All patients' data were randomly selected from the publicly available RESECT (REtroSpective Evaluation of Cerebral Tumors) database [5], which includes both pre-operative MRI and intra-operative US scans of patients with low-grade gliomas, as well as homologous anatomical landmarks for validating registration algorithms. For registration, we employed T2w FLAIR MR images, which better visualize the boundaries of the brain tumors than the T1w MR scans, and intra-operative US scans obtained before resection. The T2w FLAIR images (TE=388ms, TR=5000 ms, flip angle=120 deg., voxel size=1x1x1 mm^3, sagittal acqusition) were obtained one day before surgery on a 3T Magnetom Skyra (Siemens, Erlangen). The MRI volumes have been rigidly registered to the patient's anatomy on the surgical table. The spatially tracked US images were obtained with a sonowand Invite neuronavigation system (Sonowand AS, Trondheim, Norway), and then reconstructed as 3D volumes with resolutions range from 0.14x0.14x0.14 mm^3 to 0.24x0.24x0.24 mm^3 depending on the transducer types and imaging depths. All US volumes have full coverage of the tumors. Since the US volumes were spatially tracked during surgeries, the positions of the tissues truthfully reflect the tissue formation during the procedures. Corresponding anatomical landmarks between the MRI and US volumes were provided in the dataset for registration validation.

2.4 Registration Procedure

For each patient, we first up-sampled the MR image to the image space (and resolution) of the corresponding US images. Then, the US volumes were registered to the re-sampled MRI volumes using the technique introduced earlier. For our registration, we used a hierarchical approach, which facilitate the optimization efficiency. The registration results are reported as mean target registration errors (mTREs) for all patients under study.

2.5 Validation

In order to assess the accuracy of our method, we used the landmarks which were provided in RESECT database for each patient. Supplied landmarks can be used to calculate mean target registration error (mTRE) [10]. mTRE for a patient is defined as Eq. 16.

$$mTRE = \frac{1}{N}\sum_{i=1}^{N} \|\boldsymbol{T}(\boldsymbol{x_i}) - \boldsymbol{x_i'}\| \tag{16}$$

Where $\boldsymbol{x_i}$ and $\boldsymbol{x_i'}$ are two corresponding landmarks in moving image (US in our case) and fixed image respectively. In Eq. 16, N is the total number of landmarks.

3 Results

After image registration, we have observed an improvement in terms of image feature correspondence. From Fig. 1 and 2, we can see that borders of tumors (blue arrows) and sulci (green arrows) have been visibly re-aligned between the MR and US images. The detailed mTRE evaluation for each patient is shown in Table 1. Figure 3 depicts mTRE values before and after registration as well. Both in Table 1 and Fig. 3, we observe that mTRE values decreased after registration. Moreover, it is instructive to compare mean and standard deviation of mTRE values before registration with ones after registration. In Table 1, we can see not only the mean value but also the standard deviation decreased.

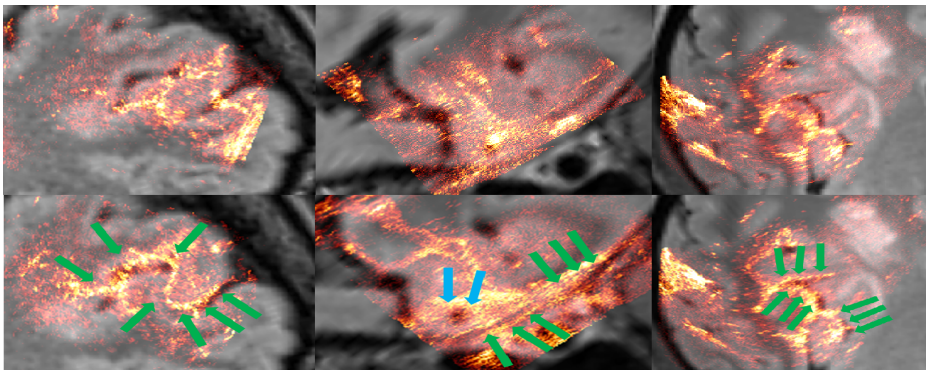

Fig. 1: Overlay of MR and US before and after registration for patient one, two, and three. First row is before registration and second row is after registration. Patient one, two, and three are first, second, and third column respectively. Green arrows correspond to sulcus and blue arrows correspond to tumor borders.

4 Discussion and Future Work

Although affine transformation has much fewer parameters than non-linear deformation, and thus may not fully represent the underlying soft tissue deformation, a few reasons justify the use of affine transformation for the demonstrated

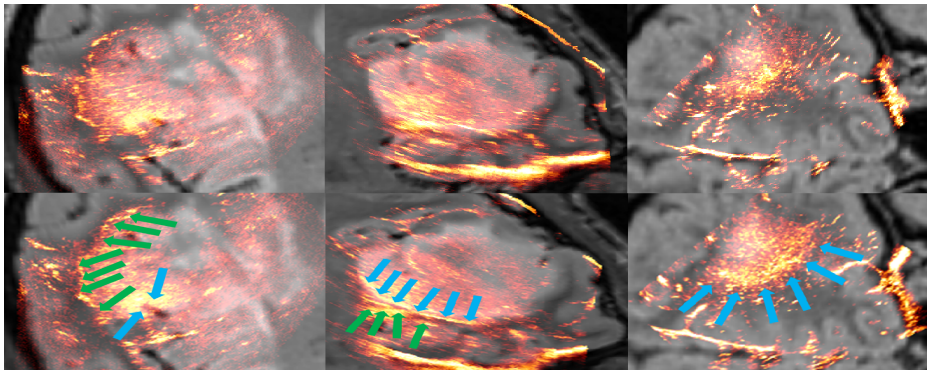

Fig. 2: Overlay of MR and US before and after registration for another view of patient three, four, and five. First row is before registration and second row is after registration. Patient three, four, and five are first, second, and third column respectively. Green arrows correspond to sulcus and blue arrows correspond to tumor borders.

Table 1: mTRE before and after registration

Patients No.	Initial mTRE	Final mTRE	No. of Landmarks
1	5.72	2.86	15
2	9.58	3.21	15
3	2.65	1.79	15
4	4.70	2.14	15
5	2.99	1.62	15
mean	5.13	2.32	
std	2.78	0.68	

application. First, as important factors in the clinic, affine registration is often faster and less prone to failure than nonlinear registration. Second, the US volumes used mainly cover the tumorous tissues, and thus the deformation can be approximated sufficiently well locally with affine transformation. Lastly, the tissue deformation before resection is not severe, and affine registration is often sufficient for the surgeons to navigate the surgical plans. Here, we have preliminarily demonstrated the proposed technique using five brain cancer patients, in the future, we will validate the method on more subjects from the RESECT database, as well as inter-modality registration tasks in other applications.

5 Conclusion

We have proposed an automatic affine registration method based on correlation ratio. The technique has been demonstrated retrospectively for MRI-US registration in the context of brain shift correction during low-grade brain gliomas resection. From both quantitative and qualitative assessments, our proposed method has shown to successfully realigned the intra-operative US with the pre-operative MRI scans.

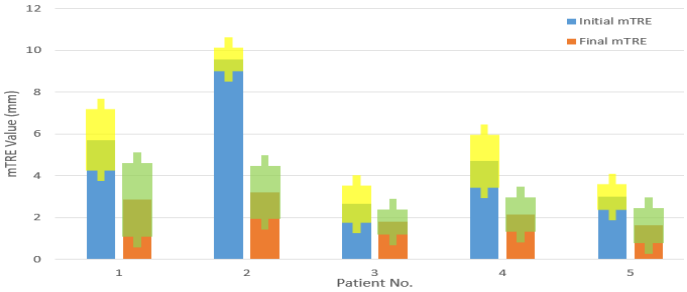

Fig. 3: Mean Target Registration Error (mTRE) Before and After Registration. Yellow and green bars indicate standard deviation before and after registration respectively.

Acknowledgements. This work is funded by Natural Science Engineering Council of Canada (NSERC) grant RGPIN-2015-04136. The authors would like to thank anonymous reviewers for their valuable feedback.

References

[1] Eric C Holland. "Progenitor cells and glioma formation". In: *Current opinion in neurology* 14.6 (2001), pp. 683–688.

[2] Therese A Dolecek et al. "CBTRUS statistical report: primary brain and central nervous system tumors diagnosed in the United States in 2005–2009". In: *Neuro-oncology* 14.suppl 5 (2012), pp. v1–v49.

[3] Ian J Gerard et al. "Brain shift in neuronavigation of brain tumors: A review". In: *Medical image analysis* 35 (2017), pp. 403–420.

[4] Dante De Nigris, D Louis Collins, and Tal Arbel. "Multi-modal image registration based on gradient orientations of minimal uncertainty". In: *IEEE transactions on medical imaging* 31.12 (2012), pp. 2343–2354.

[5] Yiming Xiao et al. "REtroSpective Evaluation of Cerebral Tumors (RESECT): a clinical database of pre-operative MRI and intra-operative ultrasound in low-grade glioma surgeries". In: *Medical Physics* (2017).

[6] Alexis Roche et al. "Multimodal image registration by maximization of the correlation ratio". PhD thesis. INRIA, 1998.

[7] Hassan Rivaz, Sean Jy-Shyang Chen, and D Louis Collins. "Automatic deformable MR-ultrasound registration for image-guided neurosurgery". In: *IEEE transactions on medical imaging* 34.2 (2015), pp. 366–380.

[8] Stefan Klein, Marius Staring, and Josien PW Pluim. "Evaluation of optimization methods for nonrigid medical image registration using mutual information and B-splines". In: *IEEE transactions on image processing* 16.12 (2007), pp. 2879–2890.

[9] Hassan Rivaz and D Louis Collins. "Near real-time robust non-rigid registration of volumetric ultrasound images for neurosurgery". In: *Ultrasound in medicine & biology* 41.2 (2015), pp. 574–587.

[10] Pankaj Daga et al. "Accurate localization of optic radiation during neurosurgery in an interventional MRI suite". In: *IEEE transactions on medical imaging* 31.4 (2012), pp. 882–891.